J. Hydrol. Hydromech., 72, 2024, 2, 238–251
https://doi.org/10.2478/johh-2024-0007

sciendo Journal of Hydrology and Hydromechanics Institute of Hydrology SAS

Varied hydrological regime of a semi-arid coastal wetland

Jaime G. Cuevas [1,2,3*], María Valladares [2,4,5], Lucas Glasner [1], Etienne Bresciani [6], Paloma Núñez [1], José L. Rojas [1], Mercedes González [1,7]

[1] Centro de Estudios Avanzados en Zonas Áridas (CEAZA), Av. Raúl Bitrán 1305, La Serena, Chile.
[2] Instituto de Ecología y Biodiversidad (IEB), Santiago, Chile.
[3] Centro de Investigación en Suelos Volcánicos (CISVo), Universidad Austral de Chile, Valdivia, Chile.
[4] Instituto de Políticas Públicas, Universidad Católica del Norte, Larrondo 1281, Coquimbo, Chile.
[5] Coastal Solutions Fellows Program, Cornell Lab of Ornithology, 159 Sapsucker Woods Road, Ithaca, NY. 14850, USA.
[6] Institute of Engineering Sciences, University of O'Higgins, Av. Libertador Gral. Bernardo O´Higgins 611, Rancagua, Chile.
[7] Universidad de La Serena, Av. Raúl Bitrán 1305, La Serena, Chile.
[*] Corresponding author. E-mail: jxcuevas@ceaza.cl

Abstract: Coastal wetlands are transitional ecosystems between land and sea. Participants of citizen science programs have detected frequent floods in wetlands, as well as small pools that appear and then disappear. Considering that it is not clear whether their main hydrologic drivers are of marine or continental origin, we studied the El Culebrón wetland located in the Chilean semi-arid zone. El Culebrón is strongly influenced by extreme rain events. This wetland also experiences seasonal changes in its water stage (WS). A high mean sea level agreed with 41% of the WS rises. High intensity storm surges coincided with 53% of WS peaks. A small tsunami in 2022 impacted the WS, and another very intense tsunami flooded it in 2015. An apparent diurnal cycle in the WS was discarded due to an instrumental artifact. The combination of the aforementioned factors provided an explanation for 91% of the WS rises. The probable and novel mechanism for sea level and storm surge influence on WS is the formation of a sand barrier between the coastal lagoon and the sea. As a whole, El Culebrón receives varied influences from both the sea and the mainland, but it seems to be more dependent on freshwater sources.

Keywords: Instrumental artifacts; Sand barrier; Diurnal cycles; Storm surges; Wetlands.

INTRODUCTION

Wetlands are environments at the interface between land and aquatic systems; they are home to diverse flora and fauna that are adapted to such conditions (Mitsch and Gosselink, 2015). Wetlands and associated landforms fulfill a role as buffers for tsunamis (Martínez et al., 2016; Rojas et al., 2015), sites for water discharge and recharge (Siegel, 1988), biofilters (López et al., 2016), and carbon dioxide sinks (Mitsch and Gosselink, 2015). They are also strategic territories due to their freshwater reserves (Gallardo and Saunders, 2018). Their significant importance in the ecosystem greatly contrasts with their conservation status because they are seriously threatened by human action, especially urban growth (Martínez et al., 2016; Rojas et al., 2015). Semi-arid coastal wetlands are even more noteworthy because they represent strikingly different conditions of moisture, plant vigor, and biodiversity, compared to the xerophytic communities found in the surrounding slopes and uplands (Contreras-López and Zuleta, 2019). Since climate change is being expressed in several places around the world with lower precipitation and higher temperatures (IPCC, 2021, p. 604), streamflows that feed wetlands are also decreasing (MMA, 2019). In fact, Hidalgo-Corrotea et al. (2023) and MMA (2019) documented that many Chilean coastal wetlands significantly reduced their extent in recent decades. Moreover, the water use of streams and aquifers for different human activities restricts the amount of freshwater feeding wetlands (Larraín and Schaeffer, 2010). All of the above coincides with the public perception that wetland sustainability is at risk by direct and indirect human actions, mainly due to the shortage of freshwater supply from streams.

On the other hand, several forcing factors from the sea may influence wetland distribution and function. For example, many coastal wetlands experience natural sea level variability caused by waves and tides (Haghani et al., 2016; Lambs et al., 2015). This influence can be relevant when waves triggered by storms in the Pacific Ocean, reach the South American coastline (Aguirre et al., 2017). These wind waves are high frequency, rhythmic oscillations that propagate across the open sea, resulting from storms and persistent winds that transfer energy and momentum across the air-sea interface. Waves can travel across entire ocean basins in the form of swells, which are wave trains born in remote or distant storms. For north-central Chile (25°S–35°S) this translates into a semi-permanent condition of a south-westerly swell that only, in unusual situations, changes to a north-west direction (Aguirre et al., 2017). It has been shown that while propagating swells lose very little energy, dissipation mainly occurs when waves reach the coast and eventually break on local shores and beaches (Munk et al., 2013; Young, 1999). The impacts of extreme waves in the Pacific south-east region (i.e., heights exceeding a specific threshold) include the coastal erosion of sandy beaches (Agredano, 2019; Martínez et al., 2018), suspension of nautical activities and port closures by local authorities, as well as coastal flooding due to storm surges and temporary sea level rises (Campos-Caba, 2016). These phenomena have intensified in recent years, with damage to coastal city infrastructures (Genovese et al., 2011; MMA, 2019), which has been linked to ongoing climate change (Vousdoukas et al., 2016). MMA (2019) has also reported breaks of sand barriers and intrusions of surges into wetlands, but as far as we are aware, no study has yet documented what type of hydrological effect storm surges have on wetlands.

The largest penetration of seawater into the mainland is associated with tsunamis, which have devastated coastal settlements in Japan, Sumatra, Hawaii, Chile, and other countries (Atwater et al., 1999; Plummer et al., 2012). The highest heights that water has been documented to reach is between 5 and 38 m above sea level, which can mean several kilometers of penetration into flat zones (Fujii et al., 2011; Liu et al., 2005). Finally, ice melting in polar regions/alpine mountains and thermosteric effects related to global warming are increasing the sea level, and prospects affirm that this phenomenon will continue (IPCC, 2021; Rahmstorf, 2007). All of these marine stressors lead to an uncertain future for wetlands. We hypothesize that in coastal semi-arid zones, forcing factors from the sea are currently more important for wetland function and subsistence than rainfall and stream discharge. This prediction could be exacerbated considering current and future climate and anthropogenic scenarios, where the spatial extent of wetlands may undergo drastic transformations. Thus, our objective was to determine the different forcing factors that are affecting wetland water levels, and their implications for the future in a typical semi-arid ecosystem.

This research arose from the observations of community members about water changes in the wetland landscape. It answers the scientific questions formulated with the participation of these local communities in citizen science program activities based on semi-arid wetlands, which the CEAZA scientific center has been running since 2015. Volunteers and collaborators participated in this research, making direct observations related to landscape changes, supporting data download campaigns, and learning about the results in workshops or meetings. Technological equipment was needed to answer the inquiries, with the final aim of supporting the scientific and social processes (Bonney, 2021).

MATERIALS AND METHODS

Study site

We worked in the El Culebrón wetland, an urban ecosystem located in the middle of Coquimbo city, Coquimbo Region, Chile (29° 57’ 43” S, 71° 19’ 19” W) (Fig. 1). The regional climate is semi-arid (Montecinos et al., 2016). Rainfall measured at 90 m a.s.l. at the La Serena meteorological station averaged 62 mm/year (period 2015–2023), with high interannual variability, while the mean temperature was 14.6 °C (2014–2023).

The wetland forms part of the 209 km^2 El Culebrón watershed (also called Pan de Azúcar) that originates from the coastal and transversal ranges of the mainland, about 25 km from the Pacific coast. The mainland is covered by xerophytic vegetation in the mountains (49.2%), agriculture (38.4%), barren land with scarce vegetation (8.1%), wetland and riparian vegetation (2.4%), and urban developments (1.9%). The coastal wetland itself is deeply constrained by urban growth. Specifically, most of the wetland is separated from the sea by a continuous highway (“Costanera”) constructed above an embankment, 2.0 m high (Fig. 1b). Moreover, a wall was constructed on the seaward side of the road to protect the embankment against surges; its foundations are several meters below ground. To the south, El Culebrón is bordered by a railway and the Baquedano neighborhood.

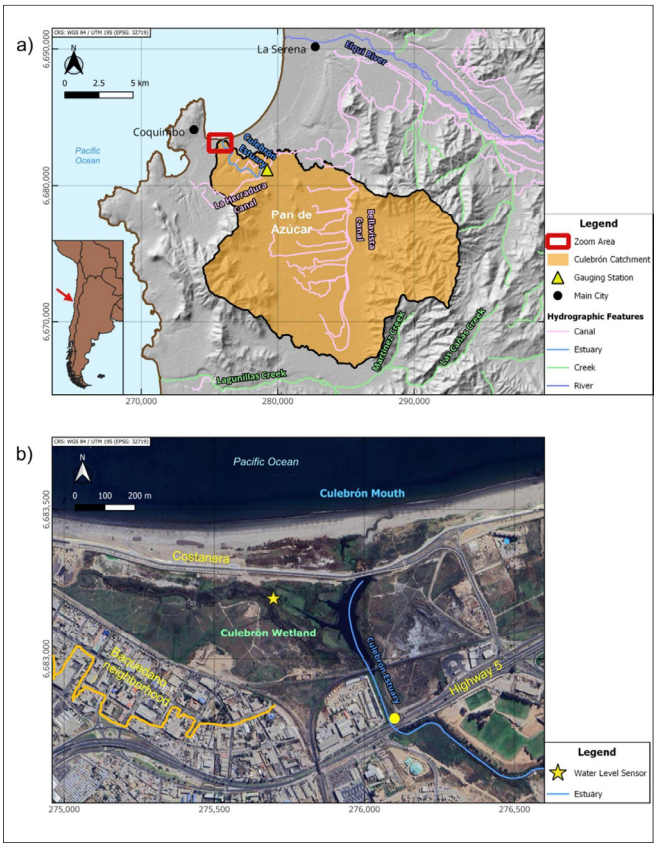

Fig. 1. a) El Culebrón watershed. b) Detail of the El Culebrón wetland. The orange line indicates the limit of the 2015 tsunami flood towards the Baquedano neighborhood, while the yellow dot points out the crossing of the El Culebrón stream under the Highway 5 bridge, where remnants of the inundation have been found.

The stream that feeds the wetland forms a coastal lagoon 350 m long, and 60 m wide that connects with the sea via a narrow outlet < 10 m wide. Usually, the surface water flow reaching the sea is restricted because there is dense plant growth (*Typha angustifolia*, narrow-leaf cattail) between the lagoon and the sea. Spot measurements of discharge at the outlet were recorded at about 0.013 m^3/s (January 2023).

The El Culebrón watershed diverts water from another major source in the Coquimbo Region called the Elqui watershed, where the Elqui River flows permanently as a result of major hydraulic interventions (Fig. 1a). The connection is provided by the Herradura and Bellavista canals, which move water for irrigation to the coastal area and the interior Pan de Azúcar sector. In this zone, the canals divide into a dense network.

Methods

Wetland water level measurements

We installed a pressure-temperature sensor in a channelled reach of the lagoon at an elevation of 1 m a.s.l. (Fig. 1b). This channel was the original outlet from the wetland to the sea, which was closed several decades ago to force the passage of water under the Costanera bridge. This channel does not have an appreciable discharge, and is approximately 1 m deep, and 5 m wide. We installed a HOBO U20-001-01-Ti pressure/temperature logger (Onset Computer Corporation, Bourne, USA) in the middle of this reach from April 2021 to April 2023. Since water was expected to be brackish, we used the titanium model. This equipment was hung from a steel cable connected to the top cap of a PVC tube perforated through its extension with 2 mm holes. The tube was kept upright with a cement base.

A barometric pressure compensation logger was placed in a sheltered garage at a 500 m distance to prevent vandalism. However, in the last months of this study the barometer was relocated to a PVC dry well surrounded by wetland water, about 20 m from the submerged sensor, following the recommendations of Cuevas et al. (2010). The device employed was a U20L-04 sensor from the same manufacturer of the other pressure transducer. Measurements were taken every 15 min.

To calculate water depth, we subtracted the barometric measurements from the submerged sensor records and divided the result by the acceleration of gravity (9.8 m/s^2), and the density of water that was collected every time we discharged the information (2–5 months). The sample was analysed in the laboratory by gravimetry and volumetry. Additionally, we installed a staff gauge 10 m from the logger location to verify the sensor linearity, and to check whether sensor drift occurred with the passing of time. This gauge was inspected every 2 – 4 months.

When estimating water depth from pressure transducers, the knowledge of the instrumental error is critical. According to the manufacturer, the typical precision errors (as defined in Rau et al. (2019), for example) are 0.5 cm and 0.4 cm for the submerged and barometric sensors, respectively, while the maximum precision errors are 1.0 cm and 0.8 cm for the same sensors. The raw pressure accuracies are 0.62 kPa and 0.43 kPa, respectively. Assuming independent errors, the precision error associated with the difference between the two records is determined as follows (Farrance and Frenkel, 2012):

a) Typical error: $\sigma_{sum} = \sqrt{0.5^2 + 0.4^2} = 0.6$ cm

b) Maximum error: $\sigma_{sum} = \sqrt{1^2 + 0.8^2} = 1.3$ cm

Cuevas et al. (2010) experimentally determined that the error in the water level estimated from two HOBO U20-001-01 pressure loggers was 0.4 cm. We also tested the two loggers in controlled conditions in the laboratory, exposed to the air, to determine the possible differences in records between them. Finally, we chose variations ≥ 2.0 cm as significant to analyse and interpret. Oscillations with a lower amplitude were considered as electronic noise.

Sea level and tide records

The variations in sea level were studied at several temporal scales. On one hand, the gravitational pull of the Sun and the Moon is associated with sea tides: full and new Moon coincide with extreme sea levels, both upwards and downwards, especially when the Moon is closer to the Earth (perigee corresponding to supermoons) (Hicks, 2006; Mitsch and Gosselink, 2015). This phenomenon manifests itself in semi-diurnal and diurnal sea level variations with amplitudes of the order of meters and phases separated by several hours. Moon calendars were accessed from the Astronomic Agenda from the Spanish Geographic Institute (https://astronomia.ign.es/rknowsys-theme/images/webAstro/paginas/documentos/Agendas_Astronomicas/Agenda_astronomica_2022.pdf). For direct records of sea level, we used information from the Chilean Navy Hydrographic and Oceanographic Service (SHOA), available by request, corresponding to Coquimbo Bay, only 2 km from our study site. Hourly records were available for the period from 2010 to the present (2023).

On the other hand, sea level also shows minor variations (decimeters), due to non-tidal processes ranging from daily to annual time scales (Pizarro et al., 2002). Thus, to distinguish the effect of tides from seasonal and other scales of variability, we performed a spectral decomposition of the sea level data into harmonic functions (sines/cosines) using Fourier methods. The seasonal cycle can be defined as the variability explained by the harmonics of the 365-day period, meanwhile tides can be defined using the harmonics of specific frequencies related to astronomical motions or "tidal constituents". In the context of sea level and tides, harmonic analysis is a common technique; for further details, the reader is referred to Pawlowicz et al. (2002). The raw sea level data was used when making comparisons on event time scales, while the daily average of the tide-filtered signal was used for seasonal and long-term comparisons.

Waves and storm surges

There is no established monitoring system for these kinds of sea level fluctuations in the Coquimbo Region. The above-mentioned SHOA monitoring does not have a temporal resolution high enough (i.e., minutes, seconds) to document changes in sea level attributable to waves and surges. Therefore, to evaluate wave heights extrema, operational wave analyses from Mercator/Météo-France model at a 1/12 degree latitude (~ 9 km) resolution were used (Alday et al., 2021). Data came from a hindcast deep-water model, and the time series represented a ~ 9 x 9 km^2 area centered at 29.917°S – 71.33°W (just in front of the El Culebrón wetland). This dataset provides recent and near real time descriptions of wave heights using a mixture of satellite observations (altimeters) and state of the art numerical models. Comparisons with independent satellite data have shown wave height errors of approximately 20 cm in mid-latitudes, meanwhile the correlation coefficient against continuous coastal buoy measurements have presented values as high as $r^2 = 0.91$ (Aouf, 2020).

This model only solves wave heights for open ocean and should not be confused with the height of waves that break on the beach, nor the sea level measured by the tide gauge. However, since surges are produced by storms spanning hundreds of

kilometers, the model resolution is adequate to describe the offshore wave field, which allows for the accurate identification of extreme regional events with coastal flooding potential. Regarding extreme wave events in central Chile, long-time numerical studies have suggested thresholds > 4.0 m for deep-water wave heights (Aguirre et al., 2017; Beyá et al., 2017). They are consistent with the satellite-based study of Mediavilla et al. (2020), which documented values of 4.5 m for the 99th percentile of wave heights off the shore of the Coquimbo Bay. Moreover, a validation of the wave model using data from Naval observations in other distant Chilean cities (Valparaíso, Talcahuano and Iquique) for the period 2022–2023, showed a good agreement between both sources ($r^2 \geq 0.88$).

We classified the storm surges as very high, high, medium, or low based on height data distribution ranges. The results obtained with the model were compared with warnings from the CEAZA and the Navy, and also with media reports from La Serena and Coquimbo, obtained from the World Wide Web. These are mainly newspaper articles and, despite the lack of scientific evaluations, they provide a rough validation of the model results, with descriptions of the largest events by local people and journalists. In addition, some field inspections carried out by the research team permitted the detection of storm surges in real time.

Additional sources of information

Meteorological information was obtained from the Ceaza-Met meteorological service belonging to the CEAZA (https://www.ceazamet.cl). The nearest station to the El Culebrón wetland is La Serena, less than 10 km away, which was consulted mainly for rainfall information.

The only stream gauging station for the El Culebrón stream itself (called The Syphon, Fig.1a) was operative between 1986 and 2017. This was located *ca.* 6 km upstream from the sea. No present gauging data is available, but we consulted old records from https://snia.mop.gob.cl/BNAConsultas/reportes (also processed at http://camels.cr2.cl/).

We also downloaded photos from Google Earth Pro Imagery, version 7.3.6.9345, for those dates when no visits to the wetland were carried out, allowing a historical comparison of its hydrological and geomorphological conditions. Finally, data from recent tsunamis were obtained from bibliographic sources (Contreras-López et al., 2016; Paleczek-Alcayaga et al., 2019).

RESULTS

Fig. 2a shows the 2-year complete series of wetland water level fluctuations. They have a baseline of about 90 cm above the streambed, with several peaks that depart from the baseline. Fluctuations are individualized by capital letters for main events, and in the following they are described from the highest to the lowest magnitudes. Table 1 shows the 22 significant effects detected, arranged by date.

Major fluctuations

In Fig. 2a, we included the daily rainfall to associate the wetland depth peaks with precipitation events. Peaks D, R and S reasonably matched with the rain events of 12.3 (June 23, 2021), 22.3 (July 10, 2022), 33.3 (July 14, 2022) and 25.9 (July 15, 2022) mm/day, respectively. In particular, the S event was the largest detected, causing a rise in the wetland water stage (WS)

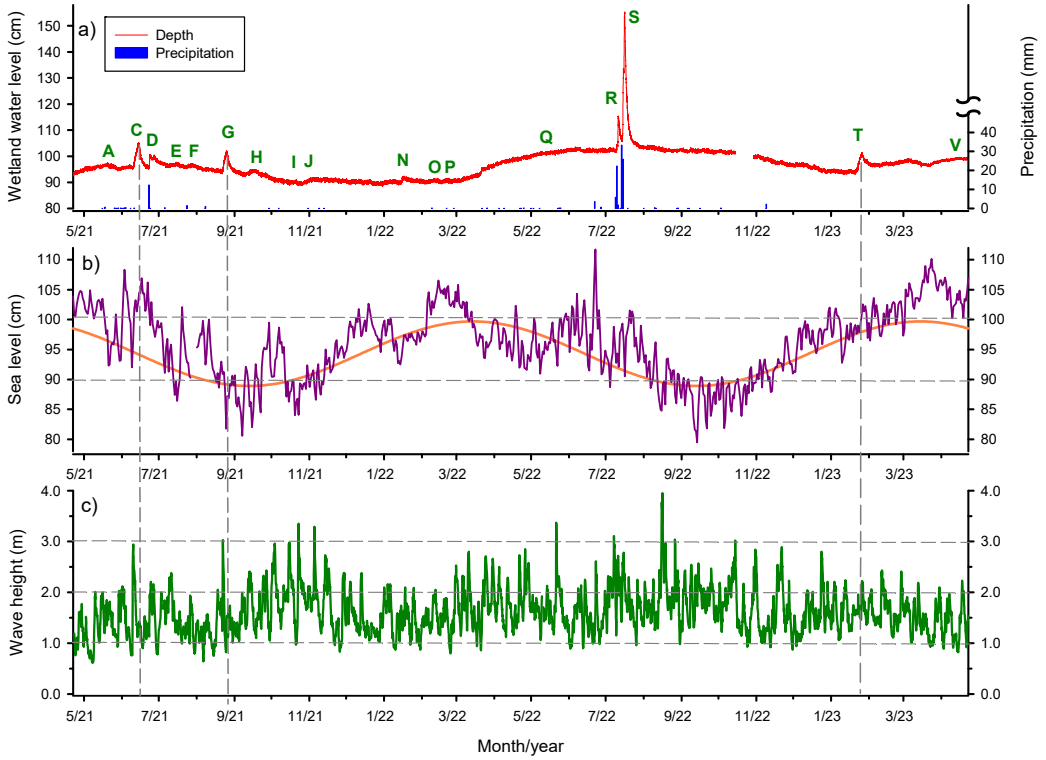

Fig. 2. a) Complete data series showing the wetland water level fluctuations, jointly explained by the daily precipitation (blue bars). Most significant peaks in the water stage at the scale of the graph are indicated by capital letters. b) Sea level fluctuations (daily means in purple, and annual harmonic in orange). c) Modelled wave height. Horizontal dashed lines separate zones of low, medium, high and very high sea level and wave height. Vertical dashed lines are used to facilitate the comparison of a), b) and c) in wetland rises of medium magnitude (peaks C, G, T).

Table 1. List of events of stage rise for the El Culebrón wetland, Coquimbo. Those with a larger magnitude and/or most likely explained are indicated with bold letters.

Event ID	Start date	End date	Peak date and time	Amplitude (cm)	Moon phase[a] at the WS peak	Mean sea level (cm) and category[b] at the WS peak	Wave height (m) and category[c] at the WS peak	Media reports for storm surges	Probable cause of event
A	4-22-21	5-28-21	5-20-21 8:00 h	5.0	1 d after CQ	98.2 M	_	_	Seasonal rise in WS
B	5-28-21	6-9-21	6-7-21 9:15 h	2.2	3 d before NM	100.3 M	1.0 M	5-28-21 warning	Moon phase/storm surge
C	**6-9-21**	**6-22-21**	**6-14-21 9:45 h**	**10.1**	**Between NM and CQ**	**102.7 H**	**1.4 M, 4 d after a HP (2.9)**	**6-10-21 reported strong**	**Mean sea level/ storm surge**
D	**6-22-21**	**7-9-21**	**6-23-21 21:45 h**	**5.6**	**1 d before FM and SM**	**101.8 H**	**2.0 H**	**6-23-21 surges 40 km to the south**	**Rain/Moon phase/mean sea level/storm surge**
E	7-9-21	7-23-21	7-15-21 7:30 h	2.2	2 d before CQ	89.7 L	1.4 M	No	Unknown
F	7-23-21	8-21-21	7-27-21 7:45 h	2.0	3 d after FM	90.3 M	1.8 M	No	Unknown
G	**8-21-21**	**9-9-21**	**8-25-21 7:30 h**	**8.9**	**3 d after FM**	**81.8 L**	**1.4 M, 3 d after a VP (3.0)**	**8-21,22-2021 reported strong**	**Moon phase/storm surge**
H	9-9-21	10-15-21	9-14-21 8:45 h	2.8	1 d after CQ	86.2 L	2.1 H	9-(10,11,12)-2021 warning	Storm surge
I	10-15-21	10-22-21	10-21-21 2:45 h	2.0	1 d after FM	86.2 L	1.0 M, 6 d after a VP (3.0)	No	Moon phase/storm surge
J	10-22-21	11-24-21	11-4-21 6:00 h	3.1	NM	91.5 M	2.0 H, 17 h before a VP (3.3)	No	Moon phase/storm surge
K	12-8-21	12-14-21	12-11-21 6:45 h	2.1	CQ	101.8 H	1.2 M	No	Mean sea level
L	12-14-21	12-22-21	12-20-21 6:30 h	2.0	1 d after FM	101.5 H	1.1 M	No	Moon phase/mean sea level
M	12-30-21	1-12-22	1-6-22 5:45 h	2.3	Between NM and CQ	100.1 M	2.0 H	1-6-22 warning	Storm surge
N	**1-15-22**	**1-24-22**	**1-16-22 4:00 h**	**2.3**	**2 d before FM**	**95.7 M**	**1.3 M**	**No**	**Tsunami/Moon phase**
O	2-5-2022	2-16-22	2-10-22 6:15 h	2.0	2 d after CQ	101.9 H	1.9 M	No	Mean sea level
P	2-16-22	2-24-22	2-22-22 7:45 h	2.1	1 d before LQ	105.6 H	1.3 M	No	Mean sea level
Q	**2-24-22**	**7-9-22**	**7-4-22 8:30 h**	**13.4**	**3 d before CQ**	**88.7 L**	_	_	**Seasonal rise in WS**
R	**7-9-22**	**7-14-22**	**7-11-22 6:45 h**	**13.8**	**2 d before FM, SM**	**92.1 M**	**2.4 H**	**No**	**Rain/Moon phase/storm surge**
S	**7-14-22**	**7-28-22**	**7-16-22 8:30 h**	**49.5**	**3 d after FM, SM**	**90.5 M**	**2.1 H**	**7-14-22 surge reports**	**Rain/Moon phase/storm surge**
T	**1-20-23**	**2-3-23**	**1-26-23 11:00 h**	**8.1**	**2 d before CQ**	**102.6 H**	**2.2 H**	**1-(18 to 23)-2023 reported strong**	**Mean sea level/storm surge**
U	2-9-23	3-14-23	3-4-23 7:45 h	3.2	3 d before FM	103.9 H, 1 d before 106.1 H	1.7 M	Warnings 2-(10 to 12, 15,16, 25)-2023	Mean sea level/storm surge
V	3-21-23	4-22-23	4-22-23 16:15 h	3.5	2 d after NM	106.9 H	_	_	Seasonal rise in WS
Summary					12 events (55%) close to NM or FM	9 H, 8 M, 5 L	7 H, 12 M 0 L	9 warnings or reports, 10 no reports	4 Moon phase/surges; 3 mean sea level/surges; 3 mean sea level; 3 mostly rain; 3 seasonal rises; 2 storm surges; 1 Moon phase/mean sea level; 1 mostly tsunami; 2 unknown.

[a] Moon phase: FM, full moon; NM, new moon; CQ, crescent quarter; LQ, last quarter; SM, supermoon. d = days, WS =wetland water stage.
[b] Mean sea level: H = high (101–112 cm), M= medium (90–<101 cm), L = low (79–<90 cm).
[c] Storm surge amplitude: V = very high (≥ 3.0 m), H = high (2.0–<3.0 m), M = medium (1–<2.0 m), L= low (< 1.0 m). P: peak, d: day, h: hour.

of up to 155 cm. In all cases, the water level peak occurred several hours after the maximum rainfall, with a lag time between the mid-point of rainfall and maximum WS of 9:15–11:15 h. However, for the S episode, the lag time was 32:30 h. These results were coherent with observations of floods in the city lowlands (Fig. 3). Light rain, as observed on June 22, 2022 (3.6 mm) failed to produce any detectable rise in water level.

A seasonal pattern was observed; the water level started at *ca.* 90 cm in April 2021, increased some centimeters by mid-May (A event, disregarding the peaks), and then returned to 90 cm during the austral spring and summer (Fig. 2a). This was even clearer in the year 2022, as the water depth increased to >100 cm in the autumn (Q "event" in Fig. 2a) and decreased in the spring. This seasonality was appreciable in the field as temporary pools formed (Fig. 4).

Medium scale variations

We attempted to correlate other wetland peaks with sea level variations, both from tides, mean levels, and storm surges. First, we studied the Moon phases as a proxy of sea level. We found that 55% of the flood events were close to full or new Moons (Table 1). The consideration of close moments and not only those corresponding to WS peaks is justified because the hydrological system is not expected to respond instantaneously to forcing factors. Then, we looked at the sea level variations, which were averaged on a daily basis to suppress the tidal cycle (Fig. 2b). The sea level was higher in the autumn of 2021, and then decreased throughout the winter to then recover during spring and summer (Fig. 2b). Maximum values were observed again at the end of February 2022, and then a decrease to the end of April 2022 was found. After that, a reduction was observed towards late winter, though there was a temporary increase in June 2022 (Fig. 2b). From the spring of 2022, the sea level increased until almost the end of the analysed record (April 2023). These trends are seen more clearly when looking at the annual harmonic superimposed onto Fig. 2b (orange line). According to Table 1, out of the 22 flood events included, 9 (41%) occurred during high mean sea level, 8 (36%) during medium sea levels, and 5 (23%) during the low sea stage.

In general, the literature evaluates swells based on characteristics of deep-water waves (100 km offshore), thus we carried out a brief analysis of the waves in the Coquimbo Bay and further from the coast (73°W – 30°S). This analysis (data not shown)

Fig. 3. Flood observed at a coastal location 3 km from the El Culebrón wetland (El Pueblito de Peñuelas, Coquimbo; July 16, 2022). Picture: Jaime Cuevas.

Fig. 4. Temporary pool on the west side of the El Culebrón wetland. Picture from October 11, 2023 (Jaime Cuevas).

demonstrated that in the wetland flood events of June 14 and August 25, 2021 (C and G events, respectively), the wave heights in the open sea were slightly higher than the 99 percentile of the historical data, which according to observations by other authors (Mediavilla et al., 2020) and the model itself is ~ 4.5–4.6 m for the region. Likewise, in the coastal zone, wave heights close to 3 m were estimated for the events in question, which are also close to the 99 percentile of the coastal time series (i.e., those heights are only surpassed 1% of the time). Overall, for the study period, the swell amplitude fluctuated between 0.6 and 4.0 m, with a mean value of 1.6 m (Fig. 2c). The highest values tended to occur in the spring. We found that 7 (37%) surges were high when the WS was also at a peak, and 12 were medium (63%) (Table 1). However, considering that three events (C, G, I) were close to high or very high surge peaks, the coincidence of major events can reach 53%. We did not evaluate the A, Q and V events because they were clearly monotonic ascents that lasted more than a month and cannot be associated with a particular sea level disturbance.

Finally, the revision of media reports concluded that only 47% of the total flood events (22) were forecasted or effectively reported as storm surges (Table 1).

Small variations

When further inspecting the record, we detected a small "notch" in mid-January, 2022 N event (Fig 2.a). When an extension of the scale was applied, a discontinuity in the record expressed as a 2.3 cm increase from 15:45 h (January 15) to 4:00 h (January 16) (UTC- 4) was indeed detected (Fig. 5). This break interrupted a sinusoidal pattern observed before/after January 15/16. The water level recovered its previous values on January 24th. We related this pattern to the Tonga submarine volcano eruption located in the Pacific Ocean, *ca.* 10,000 km from the El Culebrón wetland. According to official reports (https://www.ngdc.noaa.gov/hazel/view/hazards/tsunami/runup-data?sourceMaxYear=2022&sourceMinYear=2022&sourceCountry=TONGA), its main eruption took place on January 15th, at 4:14 h (UTC) (0:14 h, Chilean mainland time, UTC-4). Television reports indicated that the first waves hit the Chilean Coast at 15:30–16:00 h (UTC-4) (19:30–20:00 h, UTC), that is, 15–16 h after the eruption. Therefore, there is a close correspondence in the timing of direct observations and our instrumental records. We also inspected the records from the Coquimbo port, supplied by SHOA (Fig. 6). These showed the usual pattern for a semi-diurnal cycle of sea tides until January 14th. On January 15th low-high-low tides occurred normally and alternately at 3:00, 9:00, and 15:00 h, but afterwards the next high tide (155 cm) occurred in advance, at 18:00 h. Afterwards, the tide decreased abruptly to 46 cm at 19:00 h, then returned to 153 cm by 20:00 h and continued to be high until 0:00 h (January 16). Although the record tended to return to normality during the following hours, it showed a sharp pattern, i.e., after the decreases there were small increases that interrupted the continuity of the record (Fig. 6). Conversely, the increases in tide were interrupted by small diminutions. Therefore, the record was not as clean as before January 15th, suggesting that the Tonga tsunami did indeed affect the Chilean Coast. The anomaly in sea tides extended up to January 18th, three days after the main eruption.

Even stronger tsunamis have previously affected the Coquimbo coast. Although water level sensors were not installed until the year 2021, the September 16, 2015 tsunami that flooded Coquimbo city with a wave estimated at +4.5 m was well documented (Contreras-López et al., 2016). Figure 1b shows the estimated flood area in the Baquedano neighborhood, denoted by the accumulation of wet sediments and water (orange line). This tsunami also entered the El Culebrón stream, up to 2 km inland. In fact, under the Highway 5 bridge we found *T. angustifolia* debris hanging on the bridge piers (Fig. 1b, yellow dot).

Very small variations

High frequency, low-amplitude variations were also present, though they were almost invisible at the scale used in Fig. 2a. When increasing the scale, a roughly sinusoidal pattern appeared (Fig. 7a). The variation presented a maximum and minimum each day, i.e., a diurnal pattern with maxima at dawn or in the early morning (4:30–9:30 am), and minima in the afternoon (1:45–6:15 pm). The oscillation amplitude was 0.8–2.0 cm. However, before deploying loggers in the field, such a diurnal pattern already existed (Fig. 7b). Its amplitude was 0.9–1.4 cm, with maxima and minima at 4:45–9:45 am and 5:15–6:30 pm, respectively. Thus, it is likely that we are observing an instrumental artifact. As support for this possibility, when relocating the barometer to conditions similar to those experienced by the submerged logger (but exposed to the air), the daily variations changed to 0.7–1.2 cm amplitude, weaker than the laboratory conditions, and without any clear periodicity (Fig. 7c).

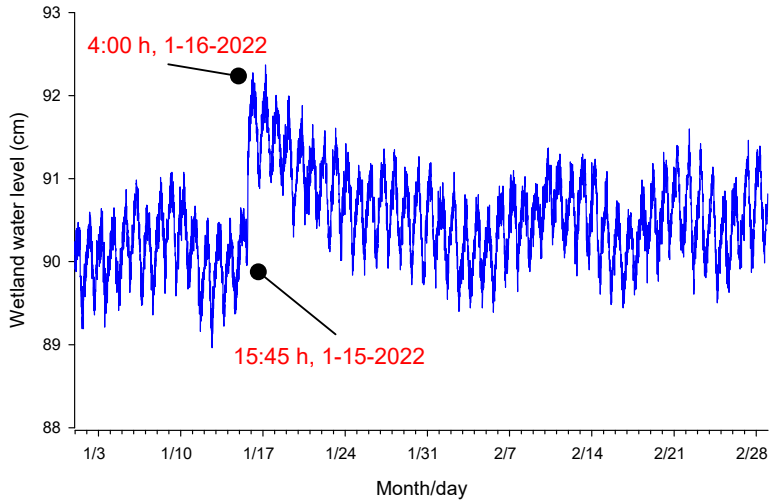

Fig. 5. Wetland water level for the summer of 2022, indicating the occurrence of a small tsunami on the Coquimbo coast.

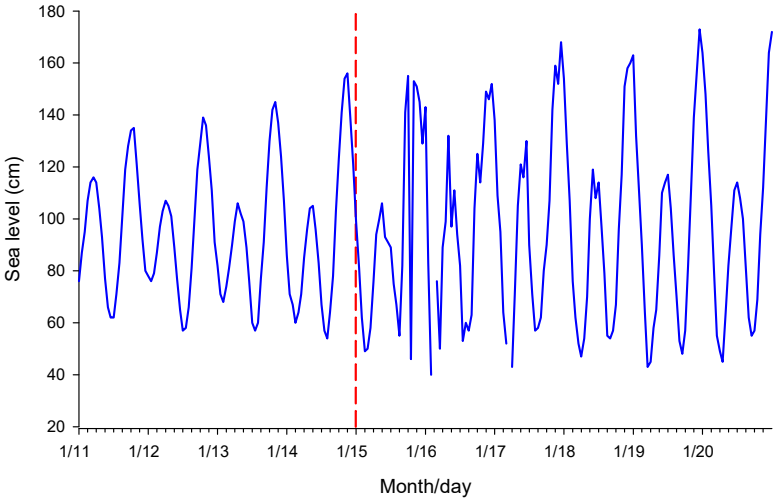

Fig. 6. Sea level variations before and after January 15, 2022, separated by the red line, when the tsunami occurred (SHOA's data).

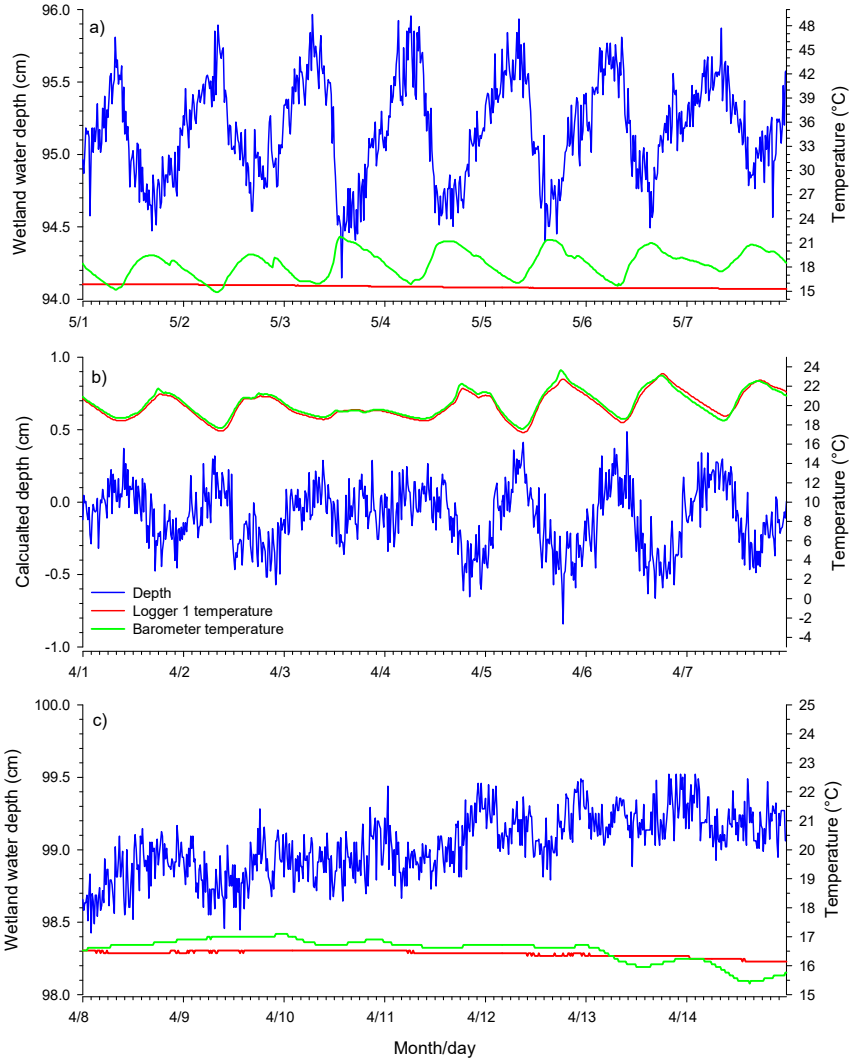

Fig. 7. Fine scale variations in water depth for the El Culebrón wetland. a) Logger number 1 was placed underwater in the wetland, while the barometer was placed at 500 m in a sheltered garage. b) Both pressure transducers were placed adjacent to each other in the laboratory, to characterize their behaviour under controlled conditions. c) Same as a), but the barometer was relocated to a dry well close to submerged logger 1. The variations in temperature for each device are also indicated. a) and b) correspond to the year 2021, while c) corresponds to the year 2023.

Considering all the above-mentioned evidence, and the declared instrumental error by the manufacturer, a 2.0 cm threshold seemed to be appropriate to discriminate between real versus noise variations.

Analysis of wetland images

At both the start and end of this study, the wetland was connected to the sea via a narrow stream between the sea and a small pool north of the Costanera bridge (Figs. 8 a, c). However, on August 24th, 2021 a sand barrier appeared, separating the pool from the sea (Fig. 8b). The wet sand suggested that the stream tried to follow its course into the sea. This date was close to the full Moon and coincided with a high wetland stage (Fig. 2a, G event) and a high modelled peak in storm surges, which was confirmed in related media reports (Table 1). Unfortunately, we did not visit the wetland on this date and could therefore not confirm this event.

On September 2nd, 2023, after the period reported in this paper, we returned to the stream mouth and discovered the reformation of the sand barrier, which once again coincided with modelled storm surge peaks, media reports, and increases in the WS (Figs. 9 a, b). This pattern did not occur in periods without increases in the WS, when surges were just beginning (previous to event T, Figs. 9 c, d). Thus, these water level rises appear to be caused by surges via the formation of a sand barrier (example events: C, G).

Integrated analysis

Considering the evidence of rainfall, Moon phases, mean sea level, tsunamis, modelled surges, and reported surges by media, we assigned each one of the flood events to probable drivers (Table 1). Accordingly, the most common pattern was four Moon phases combined with surges (18.2%). Three (13.6%) WS rises could be explained solely by a high mean sea level; three mostly by rain (even though in these events they coincided with Moon phases, sea level or storm surges); three by seasonal rises in WS; three by sea level rise/surges; two by storm surges only; one by Moon phase/sea level; and one mostly by tsunami (close to a full Moon). Considering that two events remained unexplained, 91% of them could thus be assigned a driving factor(s).

Despite a reasonable explanation for most of the 22 analysed floods, some peaks in sea level did not correspond with WS rises; for instance, June 22nd, 2022, which was the maximum recorded sea level, and a high peak in surges (Figs. 2b, c). Likewise, the absolute maximum in storm surge height observed on August 16th, 2022, also had no effect on WS.

DISCUSSION

Mitsch and Gosselink (2015) classified the hydrological behaviour of wetlands into 14 types, regarding their hydroperiods, where each wetland showed a characteristic pattern and only one or two predominant influences. In this study, we found that El Culebrón showed six variation modes, highlighting the particularity of this ecosystem. More specifically, we determined that the hydrologic behaviour of El Culebrón was strongly influenced by extreme rain events, seasonal changes in water stage, the effect of high sea tides (i.e., Moon phases), mean sea level, storm surges, and small and large tsunamis.

Rainfall effects

The lag between the mid-point of rainfall time and the maximum WS (9.25–32.5 hours) was expected in El Culebrón because the watershed is large enough to generate a delay in the water travel time from the headwaters to the watershed outlet, a delay

Fig. 8. The wetland outlet at the start (a), in the middle (b), and the end of this study (c). In a) and c), the stream mouth clearly connects to the sea at the upper extreme of the pictures, while in b) the outlet is blocked by a sand barrier. The arrows indicate the position of the small pool to the north of the Costanera bridge, which is also shown in Fig. 9. Pictures are from Google Earth Pro imagery.

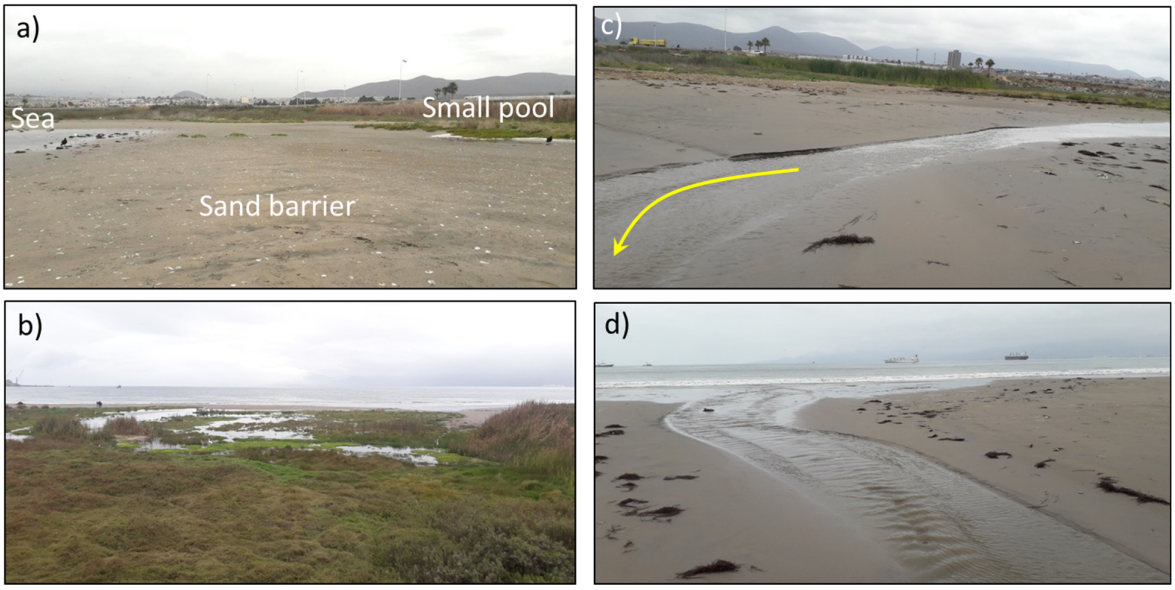

Fig. 9. a) The outlet of the El Culebrón stream on September 2nd, 2023, a few days after the closure of the sand barrier as a consequence of intense storm surges, which increased the wetland stage. In b), the flood of the small pool shown in Figures 8 a, b, c, is indicated. c) and d) Stream mouth on January 19th, 2023, when the wetland stage was decreasing and surges were just beginning. The yellow arrow indicates the flow direction. Pictures: María Valladares and Jaime Cuevas.

expressed in the parameters of time of concentration and lag time (Cuevas et al., 2019). The flood observed in the lowlands (Fig. 3) is representative of the hydrologic behaviour of El Culebrón because the entire coastal zone was a vast wetland previous to its drainage in the 1950s (Paleczek-Alcayaga et al., 2019). When extreme rainfall events occur, water flows down the steep streets of Coquimbo and La Serena and converges in the lowland wetlands. The hydraulic gradient between the wetlands and the sea of this area is small. The groundwater is also very close to the ground level and when rainfall is intense, the phreatic level rises, and groundwater movement from the uplands may also increase, contributing more water to the lowlands. In either case, the fundamental cause of these inundations is extreme rain.

Seasonal fluctuations

The observed seasonal pattern showed increases in the more humid and cooler seasons, and diminutions in the drier and warmer seasons. This is the typical behaviour of most Chilean streams originating in coastal watersheds fed by rain (Little et al., 2014). Discounting the rainfall effect, the other alternative is a larger water input from the El Culebrón stream in autumn and winter. Unfortunately, the only gauging station upstream has not been operative since the year 2017. Notwithstanding, we revised old records and found that discharges were higher in autumn and winter. In most years, this behaviour was not related to the rainfall events, which were typically < 5 per year and very variable from one year to another. This study could not verify whether the Bellavista Canal contributed surface water to the El Culebrón stream, except under extreme temporal events. This could be restricted by the fact that most of this water is used for agriculture. La Herradura canal, which also receives water from the Bellavista Canal, does indeed cross the El Culebrón ravine through a hydraulic syphon (Fig. 1a). Authors' observations have detected a seepage of this structure towards the El Culebrón stream, contributing a small discharge estimated at < 0.002 m^3/s in a nearby downstream location. It is also possible that the end of the irrigation season permits the recharge of the El Culebrón aquifer under the Pan de Azúcar valley (Fig. 1a). In support of this hypothesis, Ingeorec (2011) based on isotopic studies, indicated that 80–90% of El Culebrón water originates from the Bellavista Canal, due to irrigation spills or leakage from the canal to the aquifer followed by seepage springs. The remaining 10–20% could be attributed to local recharge from precipitation or contributions from the Lagunillas aquifer to the south of the El Culebrón aquifer. Finally, evapotranspiration by wetland plants, expected to be higher in warm seasons, could also decrease discharge.

Sea tides, mean sea level, and storm surges

As a first analysis, we considered the Moon phases as a proxy of high sea level that could influence the WS. Thus, 55% of floods were close to a full or new Moon. Although this percentage seems significant, its predictive value is low if we consider that in two years there are 24 full Moons and 24 new Moons, resulting in 48 episodes in which one could expect a wetland flood if this were the only hydrological driver. After all, the wetland did not show a semi-diurnal cycle as does the sea. Considering that we found coincidence in this regard in only 12 cases, we refined the analysis to inspect the mean sea level on the corresponding dates, to evaluate seasonal and annual trends, which were similar to those reported by Contreras-López and Zuleta (2019). Accordingly, we found that it was high in 41% of the cases, but not necessarily coinciding exactly with the Moon phases.

The degree of coincidence of large storm surges, media reports, oceanographic warnings and WS reached up to 53%. This percentage could be even higher because there is a likely bias to inform only strong surges in media reports. Notwithstanding, when this information is used jointly with other meteorological and hydrological sources, and observations of the research team, 91% of the WS rises were reasonably explained.

Not all high sea levels and large storm surges coincided with a high WS. It is possible that a wetland with a high base flow in winter is less sensitive to sea disturbances. Moreover, more

research is needed to characterize the wave features in terms of energy, direction and sediment transport to understand how they affect inland water levels.

Tsunamis

We detected the tsunami caused by the huge January 2022 volcanic explosion in Tonga. This tsunami arrived as a small flood to the Coquimbo port that did not noticeably alter its sea level record in its maximum amplitude, which is mainly controlled by sea tides. Most likely with a temporal resolution better than 1 hour, we could have obtained a clearer tsunami signal. Notwithstanding, the sea level behaved abnormally during the hours and days following the eruption. In the wetland location, the event was expressed as a sudden rise that took nine days to return to the pre-tsunami level.

The previous tsunami in this wetland (2015), and its effects on the city, have already been well described by Contreras-López et al. (2016), Contreras-López and Zuleta (2019), and Paulik et al. (2021). Another minor tsunami originating in Tohoku, Japan, arrived to the El Culebrón coast in 2011 (Paleczek-Alcayaga et al., 2019). Hence, three tsunamis have affected the area in 12 years. Traditionally, wetlands have been considered as a buffer against floods coming from the sea (Martínez et al., 2016; Rojas et al., 2015). Our evidence supports this statement when tsunamis are small, but when they are in the medium to large category, they can encroach on populated zones located several hundreds of meters inland (Atwater et al., 1999).

Daily cycles in water level

At first sight, the diurnal fluctuations observed in El Culebrón may be attributable to daily cycles of evapotranspiration that cause the wetland WS to fluctuate as a function of air temperature, as previously observed elsewhere (Carlson Mazur et al., 2014; Graham et al., 2013; Gribovszki et al., 2008). However, in our study, we proved that this is an instrumental artifact (see the Very small variations section under Results). This artifact is attributed to the difference in exposure temperature between atmospheric and water pressure transducers, and the dependence of pressure transducer measurements on temperature (Cuevas et al., 2010; McLaughlin and Cohen, 2011; Rau et al., 2019).

If a daily evaporative cycle exists in our wetland, its amplitude must be smaller than 2 cm, and its observation would require more accurate instruments. In any case, our results demonstrate that carefully analysing instrumental capabilities is essential. Unfortunately, many articles do not provide enough information about the location, testing of behaviour of instruments *prior* to deployment, and/or quantification of measurement errors, which are critical issues when documenting diel signals and the estimation of evapotranspiration by analysing variations in WS.

Pathways for wetland water level variations

When influences come from rain or via streams it is clear that a surface connection between the wetland and its water sources exists. However, the influence from the sea is more difficult to trace because we have not observed its invasion, except when tsunamis occur (2015 and 2011, see also Paleczek-Alcayaga et al., 2019). The measured flood due to the Tonga volcanic eruption in 2022 also, most likely, implied the entrance of surface seawater into the wetland, as concluded from the sudden rise in the hydrograph (Fig. 5). Most of the time, the separation between this wetland and the beach by a continuous highway constructed above an embankment, and the underground wall on the seaward side of the road, make it difficult for sea water to enter the coastal lagoon. In fact, this was the reason for constructing the wall, whose foundations lie 2.0–3.0 m below the wetland ground level (according to the manufacturer). Therefore, the main interaction between marine and wetland waters should occur under the Costanera bridge (Fig. 1b) (besides a few small culverts under the Costanera). Notwithstanding, this outlet is covered by dense growth of *T. angustifolia,* which makes both the entrance and exit of water difficult. Groundwater interconnection between the sea and the wetland might produce wetland floods, but no evident and permanent correlation was observed between mean sea level and WS, in spite of the fact that Asistecsa (2017) found permeable strata (silt and sand) up to 15 m belowground. Additional measurements are needed to support this hypothesis. However, we have noted that, especially in storm surge events, a sand barrier appears downstream from the Costanera bridge, separating the stream from the sea. The influence that this barrier has on the WS was also supported by the observation of the hydrograph shapes (Fig. 10): they have rounded ascending and falling limbs, with several days to reach the peak and then return to the base level. This is a gradual flood typical of wide swamp floodplains (Cuevas et al., 2019), and very different from storm hydrographs, such as those from July 2022.

According to Haghani et al. (2016), the formation of barrier-lagoon systems due to sea level rise is quite typical in different areas of the world, but in our research, we detected an indirect effect of surges on wetland hydrology, a novel mechanism in this regard. In the Chilean setting, it was believed that surges only broke the barriers, allowing the passage of water into wetlands (Contreras-López and Zuleta, 2019). However, storm surges also apparently generate an accumulation of sand from the beach, until the mouth is closed off. Nevertheless, the highest rise in WS caused by surges was < 10 cm, which suggests that the stream can break the sand barrier after the flood, returning to discharge values similar to those prior to the formation of the barrier. Further research is required to understand the geomorphological drivers responsible for this process.

CONCLUSIONS

Our hypothesis about a dominance of marine influences on wetland hydrology was not supported because we documented a mixed hydrological regime in the studied wetland, with influences from both the sea and the mainland. Although tsunami effects were confirmed, they were sporadic compared to the floods caused by annual rainfall, seasonal trends in streamflow, and sand barrier closure, which increased freshwater storage. In this sense, the public perception is accurate to believe that wetlands are more dependent on continental water sources rather than marine sources. The sea level in this region is more likely to influence wetland stage due to tidal levels, seasonal changes, or storm surges. We detected a novel influence of storm surges on wetland hydrology, mediated by the formation of a sand barrier.

The present results on the hydrodynamics of the El Culebrón wetland provide real data for community decision-making regarding urban development. This study provides concrete answers to questions of interest to citizens, and direct observations of changes in the wetland's landscape that could occur in an extreme climate change scenario. Through the CEAZA citizen science program, environmental education among the inhabitants of this semi-arid region is undertaken regarding the effects of climate change, and the importance that wetlands have in the dynamics of the coastal zone (Núñez et al., 2019).

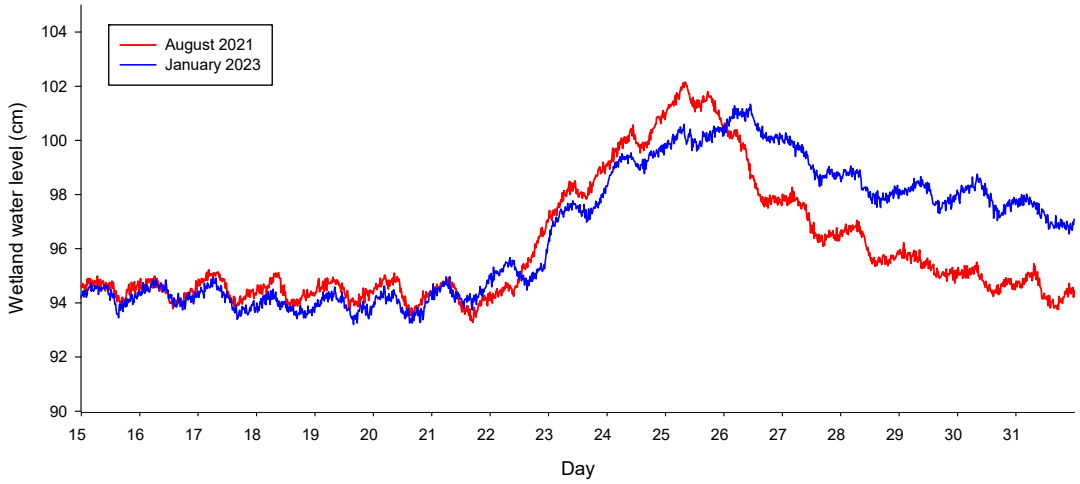

Fig. 10. Flood hydrographs associated with storm surges. The several-day span of the rising and declining water level periods supports the hypothesis of these responses being caused by the creation and subsequent opening of a sand barrier. Days correspond to calendar dates for different months.

Acknowledgements. The purchase of water level sensors was possible due to the Conicyt Project "Fortalecimiento de la generación y transferencia del conocimiento científico interdisciplinario de CEAZA, a partir de la vinculación con los territorios y ecosistemas de la región de Coquimbo 2017-2020". Monitoring was also supported by the FIC grant "Caracterización Red de Humedales Región Coquimbo" provided by the Regional Government, Coquimbo, Bip code 40043869-0. We sincerely thank these funding sources. LG and MV acknowledge support from ANID (Concurso de Fortalecimiento al Desarrollo Científico de Centros Regionales 2020-R20F0008 CLAP project-CEAZA). Project 3° Concurso de Iniciativas de Humedales Costeros y Aves Playeras 2023-2024 "Manejo Participativo de la Cuenca del Humedal El Culebrón" MAPACULEBRON also supported this initiative. The Navy Hydrographic and Oceanographic Service (SHOA) provided its valuable reports on sea tides. Moreover, CEAZA supported us with the loan of pick-up trucks. Dr. Boris Dewitte made some useful suggestions, and Palmenia Donaire, Jorge Ramírez, and Guillermo Narváez helped us in the field. Finally, the journalist Catalina Velasco contributed with the compilation of storm surge reports from the web, and two anonymous reviewers are acknowledged for their comments.

REFERENCES

Agredano, R., Cienfuegos, R., Catalán, P., Mignot, E., Bonneton, P., Bonneton, N., Martínez, C., 2019. Morphological changes in a cuspate sandy beach under persistent high-energy swells: Reñaca Beach (Chile). Mar. Geol., 417, 105988. https://doi.org/10.1016/J.MARGEO.2019.105988

Aguirre, C., Rutllant, J.A., Falvey, M., 2017. Wind waves climatology of the Southeast Pacific Ocean. Int. J. Climatol., 37, 4288–4301. https://doi.org/10.1002/joc.5084

Alday, M., Accensi, M., Ardhuin, F., Dodet, G., 2021. A global wave parameter database for geophysical applications. Part 3: Improved forcing and spectral resolution. Ocean Model. (Oxf), 166, 101848. https://doi.org/10.1016/J.OCEMOD.2021.101848

Aouf, L., 2020. Quality information document for global ocean waves analysis and forecasting product GLOBAL_ANALYSIS_FORECAST_WAV_001_027. Copernicus Marine Environment Monitoring Service, (1).

Asistecsa (Ingenieros Consultores), 2017. Estudios condiciones de suelo para conservación costanera de Coquimbo, comuna de Coquimbo, Provincia de Elqui, IV Región de Coquimbo. Santiago, Chile, 34 p.

Atwater, B.F., Cisternas, M.V, Bourgeois, J., Dudley, W.C., Hendley II, J.W., Stauffer, P.H., 1999. Surviving a tsunami: lessons from Chile, Hawaii, and Japan. U.S. Department of the Interior, U.S.G.S.; Circular 1187, 18 p. https://doi.org/10.3133/cir1187

Beyá, J., Álvarez, M., Gallardo, A., Hidalgo, H., Winckler, P., 2017. Generation and validation of the Chilean Wave Atlas database. Ocean Model. (Oxf), 116, 16–32. https://doi.org/10.1016/J.OCEMOD.2017.06.004

Bonney, R., 2021. Expanding the impact of citizen science. BioScience, 71, 5, 448–451. https://doi.org/10.1093/biosci/biab041

Campos-Caba, R., 2016. Análisis de marejadas históricas y recientes en las costas de Chile. Memoria del proyecto para optar al Título de Ingeniero Civil Oceánico. Universidad de Valparaíso, Valparaíso, Chile.

Carlson Mazur, M.L., Wiley, M.J., Wilcox, D.A., 2014. Estimating evapotranspiration and groundwater flow from water-table fluctuations for a general wetland scenario. Ecohydrology, 7, 378–390. https://doi.org/10.1002/eco.1356

Contreras-López, M., Winckler, P., Sepúlveda, I., Andaur-Álvarez, A., Cortés-Molina, F., Guerrero, C.J., Mizobe, C.E., Igualt, F., Breuer, W., Beyá, J.F., Vergara, H., Figueroa-Sterquel, R., 2016. Field survey of the 2015 Chile tsunami with emphasis on coastal wetland and conservation areas. Pure Appl. Geophys., 173, 349–367. https://doi.org/10.1007/s00024-015-1235-2

Contreras-López, M., Zuleta, C., 2019. Capítulo 7: Vulnerabilidades de los humedales costeros de Coquimbo. In: Zuleta, C., Contreras, M. (Eds.): Humedales Costeros de la Región de Coquimbo: Biodiversidad, Vulnerabilidades & Conservación. Ediciones Universidad de La Serena & Ministerio del Medio Ambiente, La Serena, Chile, pp. 183–221.

Cuevas, J.G., Calvo, M., Little, C., Pino, M., Dassori, P., 2010. Are diurnal fluctuations in streamflow real? J. Hydrol. Hydromech., 58, 149–162. https://doi.org/10.2478/v10098-010-0014-0

Cuevas, J.G., Arumí, J.L., Dörner, J., 2019. Assessing methods for the estimation of response times of stream discharge: The

role of rainfall duration. J. Hydrol. Hydromech., 67, 143–153. https://doi.org/10.2478/johh-2018-0043

Farrance, I., Frenkel, R., 2012. Uncertainty of measurement: A review of the rules for calculating uncertainty components through functional relationships. The Clinical Biochemist Reviews, 33, 49–75.

Fujii, Y., Satake, K., Sakai, S., Shinohara, M., Kanazawa, T., 2011. Tsunami source of the 2011 off the Pacific coast of Tohoku Earthquake. Earth Planets Space, 63, 815–820. https://doi.org/10.5047/eps.2011.06.010

Gallardo-Fernández, G.L., Saunders, F., 2018. Commoditization of rural lands in the semi-arid region of Chile—the case of the Huentelauquén agricultural community. Agriculture (Switzerland), 8, 26. https://doi.org/10.3390/agriculture8020026

Genovese, E., Hallegatte, S., Dumas, P., 2011. Damage assessment from storm surge to coastal cities: Lessons from the Miami Area. In: Geertman, S., Reinhardt, W., Toppen, F. (Eds.): Advancing Geoinformation Science for a Changing World. Springer-Verlag, Berlin, Heidelberg, Germany, pp. 21–43. https://doi.org/10.1007/978-3-642-19789-5_2

Graham, C.B., Barnard, H.R., Kavanagh, K.L., Mcnamara, J.P., 2013. Catchment scale controls the temporal connection of transpiration and diel fluctuations in streamflow. Hydrol. Process., 27, 2541–2556. https://doi.org/10.1002/hyp.9334

Gribovszki, Z., Kalicz, P., Szilágyi, J., Kucsara, M., 2008. Riparian zone evapotranspiration estimation from diurnal groundwater level fluctuations. J. Hydrol., 349, 6–17. https://doi.org/10.1016/j.jhydrol.2007.10.049

Haghani, S., Leroy, S.A.G., Wesselingh, F.P., Rose, N.L., 2016. Rapid evolution of coastal lagoons in response to human interference under rapid sea level change: A south Caspian Sea case study. Quatern. Int., 408, 93–112. https://doi.org/10.1016/j.quaint.2015.12.005

Hicks, S.D., 2006. Understanding tides. Center for Operational Oceanographic Products and Services, U.S. Department of Commerce, National Oceanic and Atmospheric Administration, National Ocean Service, USA, 83 p.

Hidalgo-Corrotea, C., Alaniz, A.J., Vergara, P.M., Moreira-Arce, D., Carvajal, M.A., Pacheco-Cancino, P., Espinosa, A., 2023. High vulnerability of coastal wetlands in Chile at multiple scales derived from climate change, urbanization, and exotic forest plantations. Sci. Total. Environ., 903, 166130. https://doi.org/10.1016/j.scitotenv.2023.166130

INGEOREC, 2011. Compañía minera Carmen de Andacollo, hidrogeología y modelo numérico de la cuenca costera del estero Culebrón. Segunda etapa. Santiago, Chile.

IPCC (Intergovernmental Panel on Climate Change), 2021. Climate change 2021 – The physical science basis. In: Masson-Delmotte, V., Zhai, P., Pirani, A., Connors, S.L., Péan, C., Berger, S., Caud, N., Chen, Y., Goldfarb, L., Gomis, M.I., Huang, M., Leitzell, K., Lonnoy, E., Matthews, J.B.R., Maycock, T.K., Waterfeld, T., Yelekçi, O., Yu, R., Zhou, B. (Eds.): Contribution of Working Group I to the Sixth Assessment Report of the Intergovernmental Panel on Climate Change. Cambridge University Press, Cambridge, United Kingdom and New York, NY, USA, 2391 p. https://doi.org/10.1017/9781009157896

Lambs, L., Bompy, F., Imbert, D., Corenblit, D., Dulormne, M., 2015. Seawater and freshwater circulations through coastal forested wetlands on a Caribbean Island. Water (Switzerland), 7, 4108–4128. https://doi.org/10.3390/w7084108

Larrain, S., Schaeffer, C., 2010. Conflicts over water in Chile: Between human rigths and market rules. Programa Chile Sustentable, Santiago, Chile. 58 p.

Little, C., Cuevas, J.G., Lara, A., Pino, M., Schoenholtz, S., 2014. Buffer effects of streamside native forests on water provision in watersheds dominated by exotic forest plantations. Ecohydrology, 8, 1205–1217. https://doi.org/10.1002/eco.1575

Liu, P.L.F., Lynett, P., Fernando, H., Jaffe, B.E., Fritz, H., Higman, B., Morton, R., Goff, J., Synolakis, C., 2005. Observations by the International Tsunami Survey Team in Sri Lanka. Science 308, 1595. https://doi.org/10.1126/science.1110730

López, D., Sepúlveda, M., Vidal, G., 2016. *Phragmites australis* and *Schoenoplectus californicus* in constructed wetlands: Development and nutrient uptake. J. Soil Sci. Plant Nutr., 16, 3, 763–777.

Martínez, C., Contreras-López, M., Winckler, P., Hidalgo, H., Godoy, E., Agredano, R., 2018. Coastal erosion in central Chile: A new hazard? Ocean Coast. Manag., 156, 141–155. https://doi.org/10.1016/j.ocecoaman.2017.07.011

Martínez, C., Rojas, C., Rojas, O., Quezada, J., López, P., Ruíz, V., 2016. Crecimiento urbano sobre geoformas costeras de la llanura de San Pedro, Área Metropolitana de Concepción. In: Hidalgo, R., Santana, D., Arenas, F., Salazar, A., Valdebenito, C., Álvarez, L. (Eds.): En las costas del neoliberalismo: naturaleza, urbanización y producción inmobiliaria: experiencias en Chile y Argentina. 1st ed, serie GEOlibros Nº 23, Instituto de Geografía, Pontificia Universidad Católica de Chile - Instituto de Geografía, Pontificia Universidad Católica de Valparaíso, pp. 287–312.

McLaughlin, D.L., Cohen, M.J., 2011. Thermal artifacts in measurements of fine-scale water level variation. Water Resour. Res., 47, W09601. https://doi.org/10.1029/2010WR010288.

Mediavilla, D., Sepúlveda, H.H., Alonso, G., 2020. Wind and wave height climate from two decades of altimeter records on the Chilean Coast (15°–56.5° S). Ocean Dynam., 70, 231–239. https://doi.org/10.1007/s10236-019-01316-9

Mitsch, W.J., Gosselink, J.G., 2015. Wetlands. 5th Ed. John Wiley & Sons, Inc., Hoboken, New Jersey, USA, 736 p.

MMA (Ministerio del Medio Ambiente), 2019. Volumen 6: Vulnerabilidad en humedales. In: Ministerio del Medio Ambiente (Ed.): Determinación del riesgo de los impactos del Cambio Climático en las costas de Chile. Prepared by: Winckler, P., Contreras-López, M., Vicuña, S., Larraguibel, C., Mora, J., Esparza, C., Salcedo, J., Gelcich, S., Fariña, J. M., Martínez, C., Agredano, R., Melo, O., Bambach, N., Morales, D., Marinkovic, C., Pica, A. Santiago, Chile. https://doi.org/10.13140/RG.2.2.30575.38564

Montecinos, S., Gutiérrez, J.R., López-Cortés, F., López, D., 2016. Climatic characteristics of the semi-arid Coquimbo Region in Chile. J. Arid Environ., 126, 7–11. https://doi.org/10.1016/j.jaridenv.2015.09.018

Munk, W., Miller, G., Snodgrass, F., Barber, N., 2013. Erratum: Directional recording of swell from distant storms (Philosophical Transactions of the Royal Society A: Mathematical, Physical and Engineering Sciences (1963) 255 (505–584) https://doi.org/10.1098/rsta.1963.0011). Philosophical Transactions of the Royal Society A: Mathematical, Physical and Engineering Sciences. https://doi.org/10.1098/rsta.2013.0039

Núñez-Farías, P., Velásquez-Contreras, S., Ríos-Carmona, V., Velásquez-Contreras, J., Velásquez-Contreras, M.E., Rojas-Rojas, J.L., Riveros-Flores, B., 2019. "Citizen Science Among All" Participatory Bird Monitoring of the Coastal Wetland of the Limarí River, Chile. Narrative Inquiry in Bioethics, 9, 1, E3–E8.

Paleczek-Alcayaga, H., Pizarro-Pardo, J., Bravo-Naranjo, V., Trujillo-Acosta, A., Zuleta, C., 2019. Usos y degradación de los humedales costeros de la Región de Coquimbo. In: Zuleta, C., Contreras, M. (Eds.): Humedales Costeros de la Región de

Coquimbo: Biodiversidad, Vulnerabilidades & Conservación. Ediciones Universidad de La Serena & Ministerio del Medio Ambiente, La Serena, Chile, pp. 250–277.

Paulik, R., Williams, J.H., Horspool, N., Catalan, P.A., Mowll, R., Cortés, P., Woods, R., 2021. The 16 September 2015 Illapel earthquake and tsunami: Post-event tsunami inundation, building and infrastructure damage survey in Coquimbo, Chile. Pure Appl. Geophys., 178, 4837–4851. https://doi.org/10.1007/s00024-021-02734-x

Pawlowicz, R., Beardsley, B., Lentz, S., 2002. Classical tidal harmonic analysis including error estimates in MATLAB using T_TIDE. Computers & Geosciences, 28, 8, 929–937.

Pizarro, O., Shaffer, G., Dewitte, B., Ramos, M., 2002. Dynamics of seasonal and interannual variability of the Peru-Chile Undercurrent. Geophys. Res. Lett., 29, 12, 1581.

Plummer, C.C., Carlson, D.H., Hammersley, L., 2012. Physical Geology. 14th Ed. McGraw-Hill Education, 2 Penn Plaza, New York, NY 10121, USA, 704 p.

Rahmstorf, S., 2007. A semi-empirical approach to projecting future sea-level rise. Science, 315, 368–370. https://doi.org/10.1126/science.1135456

Rau, G.C., Post, V.E.A., Shanafield, M., Krekeler, T., Banks, E.W., Blum, P., 2019. Error in hydraulic head and gradient time-series measurements: A quantitative appraisal. Hydrol. Earth Syst. Sc., 23, 3603–3629. https://doi.org/10.5194/hess-23-3603-2019

Rojas, C., Sepúlveda-Zúñiga, E., Barbosa, O., Rojas, O., Martínez, C., 2015. Patrones de urbanización en la biodiversidad de humedales urbanos en Concepción metropolitano. Rev. Geogr. Norte Gd., 61, 181–204.

Siegel, D.I., 1988. A review of the recharge-discharge function of wetlands. In: Hook, D.D., McKee, W.H., Smith, H.K., Gregory, J., Burrell, V.G., DeVoe, M.R., Sojka, R.E., Gilbert, S., Banks, R., Stolzy, L.H., Brooks, C., Matthews, T.D., Shear, T.H. (Eds.): The Ecology and Management of Wetlands, Volume 1, Ecology of Wetlands. Springer US, New York, NY, pp. 59–67. https://doi.org/10.1007/978-1-4684-8378-9_6

Vousdoukas, M.I., Voukouvalas, E., Annunziato, A., Giardino, A., Feyen, L., 2016. Projections of extreme storm surge levels along Europe. Clim. Dynam., 47, 3171–3190. https://doi.org/10.1007/s00382-016-3019-5

Young, I.R., 1999. Seasonal variability of the global ocean wind and wave climate. Int. J. Climatol., 19, 931–950. https://doi.org/10.1002/(SICI)1097-0088(199907)19:9<931::AID-JOC412>3

Received 4 December 2023
Accepted 28 February 2024